A Re-Examination of Subcarrier Demodulator Performance

J. R. Lesh
Network Operations Section

The Subcarrier Demodulator Assembly (SDA) is re-examined, and a mathematical model is developed wherein an attempt is made to remove some of the restrictions placed on previous models. The resulting model is found to differ from the previous model at low symbol rates, when subcarrier doppler offsets exist, or when carrier tracking phase errors become significant.

I. Introduction

Since its inception, the Subcarrier Demodulator Assembly (SDA) has been studied quite extensively. The most notable of these studies was performed by Brockman (Refs. 1–5). In this article the SDA is re-examined with an attempt to include the effects of

(1) SDA phase errors upon the SDA loop.

(2) Carrier tracking loop phase errors.

(3) A recent study involving the theory of soft limiters (Ref. 6).

The SDA model created in this study is then compared with the earlier Brockman model. The two models are found to deviate most when compared at low symbol rates, when subcarrier doppler offsets exist, or when carrier tracking errors are significant. For ease of comparison, the terminology used in this paper will match that used in the Brockman papers as closely as possible.

II. SDA Model

A block diagram of the data channel portion of the SDA is shown in Fig. 1. The input to the SDA is a signal of the form

$$u(t) = \sqrt{2}A \sin\{\omega_c t + m_{PS} m(t) \cos[\omega_{SC} t + \theta_{SC}(t)]\} + n(t) \quad (1)$$

Here, A represents the rms signal amplitude, ω_C is the intermediate frequency (IF) carrier angular frequency, $m(t)$ is the binary data stream, assuming values of ± 1, which biphase modulates the unit amplitude squarewave subcarrier

$$S(t) = \cos[\omega_{SC} t + \theta_{SC}(t)] \quad (2)$$

and m_{PS} is the phase modulation angle of the IF carrier. The resulting signal is then immersed in zero mean white Gaussian noise having a one-sided spectral density of

N_0 watts/Hz. This input signal is mixed with the locally generated estimate of the subcarrier signal

$$\hat{S}_D(t) = \cos[\omega_{SC}t + \hat{\theta}_{SC}(t)] \tag{3}$$

which is supplied by the error channel portion of the SDA. After bandpass filtering and mixing with the 10-MHz reference signal

$$\sqrt{2}\cos[\omega_c t + \phi_R(t)] \tag{4}$$

we have the demodulated data signal

$$A \sin m_{PS}\left(1 - \frac{2}{\pi}|\phi_{SC}(t)|\right)\cos[\phi_R(t)]\, m(t) \tag{5}$$

where

$$\phi_{SC}(t) = \theta_{SC}(t) - \theta_{SC}(t) \tag{6}$$

is the subcarrier loop phase error and $\phi_R(t)$ is the phase error of the receiver carrier tracking loop. The demodulated data signal is finally filtered and limited to produce the local estimate of the data stream $\hat{m}(t)$ for use in the error channel portion of the SDA.

Refer now to the block diagram of the error channel portion of the SDA shown in Fig. 2. The squarewave VCO produces, along with the subcarrier estimate $S_D(t)$, the quadrature estimate

$$\hat{S}_E(t) = \sin[\omega_{SC}t + \hat{\theta}_{SC}(t)] \tag{7}$$

This quadrature estimate is modulated by the local data estimate and is then mixed with the incoming signal to produce a signal $v(t)$, the amplitude of which is proportional to the subcarrier loop phase error

$$v(t) = \frac{2\sqrt{2}}{\pi} A \sin m_{PS} m(t)\, \hat{m}(t)\, \phi_{SC}(t) \cos \omega_c t + n(t) \tag{8}$$

This error signal is applied to the bandpass filter to provide the input $x(t)$ to the soft limiter. The expression for $x(t)$ is

$$x(t) = \frac{2\sqrt{2}}{\pi} A \sin m_{PS}\, \alpha'\, \phi_{SC}(t) \cos \omega_c t + n'(t) \tag{9}$$

where α' is the average of the product of $m(t)$ and $\hat{m}(t)$ and $n'(t)$ is the input noise term of one-sided spectral density N_0 but restricted to the bandwidth BW_{FA_2} (one produces, along wit hthe subcarrier estimate $S_D(t)$, the sided) of the bandpass filter. In Brockman (Ref. 5), an expression is given for α' when the symbol transition probability is 0.5 and the ratio of data lowpass filter time constant to symbol period is 1/3. This expression, however, does not include the effects of degradation from either the subcarrier loop or the carrier tracking loop. To include these effects, we can compute an effective (average) signal strength into the data channel lowpass filter by first assuming that the subcarrier and carrier tracking loop phase errors are independent. Then, if we assume that the SDA phase error is Gaussian, we have that the signal voltage reduction due to the subcarrier loop phase error is, from Brockman (Ref. 2),

$$E\left[1 - \frac{2}{\pi}|\phi_{SC}(t)|\right] = 1 - \left(\frac{2}{\pi}\right)^{3/2} \exp\left[-\left(\frac{\phi_{SCL}^2}{2\sigma_{SC}^2}\right)\right] \times \sigma_{SC} - \frac{2}{\pi}\phi_{SCL}\,\mathrm{erf}\left(\frac{\phi_{SCL}}{\sqrt{2}\,\sigma_{SC}}\right) \tag{10}$$

where ϕ_{SCL} is the mean (static) SDA phase error and σ_{SC}^2 is the SDA phase variance. For the reduction effect of the carrier loop we recall from Lindsey (Ref. 7) that when the receiver static phase error is zero,

$$E\{\cos[\phi_R(t)]\} = \frac{I_1(\rho)}{I_0(\rho)} \tag{11}$$

where $I_v(x)$ is the vth-order modified Bessel function of argument x and ρ is the carrier tracking loop signal-to-noise ratio. For the case when a static receiver phase error is nonzero, the corresponding expression is much more complex but will be approximated by

$$E\{\cos[\phi_R(t)]\} \approx \frac{I_1(\rho)}{I_0(\rho)} \cos \phi_{RL} \tag{12}$$

where ϕ_{RL} is the static phase error in the receiver loop. Using these results and defining R as the symbol energy to noise density ratio (ST_S/N_0) we have that the degraded signal-to-noise ratio R_d at the input to the data channel lowpass filter is

$$R_d = R\left\{\left[1 - \left(\frac{2}{\pi}\right)^{3/2} \exp\left(-\frac{\phi_{SCL}^2}{2\sigma_{SC}^2}\right)\sigma_{SC} - \frac{2}{\pi}\phi_{SCL}\,\mathrm{erf}\left(\frac{\phi_{SCL}}{\sqrt{2}\,\sigma_{SC}}\right)\right]^2 \times \left[\frac{I_1(\rho)}{I_0(\rho)}\cos\phi_{RL}\right]^2\right\} \tag{13}$$

and the expression for α' becomes

$$\alpha' = (0.769)\left[\frac{0.887 + 0.2\,R_d^{1.2}}{1 + 0.2\,R_d^{1.2}}\right]\operatorname{erf}\left(\sqrt{\frac{2\,R_d}{3}}\right) \tag{14}$$

Returning now to Eq. (9) and defining

$$K_1(t) = \frac{2\sqrt{2}}{\pi} A \sin m_{PS}\,\alpha' \cos \omega_c t \tag{15}$$

we see immediately that the diagram in Fig. 2 has the equivalent mathematical model shown in Fig. 3.

To proceed further with this model, we must determine the effects of the soft limiter. The limiter is assumed to have an error function transfer characteristic; that is, the output y is related to the input x by

$$y(x) = L \operatorname{erf}\left(\frac{C\sqrt{\pi}}{2L}\,x\right) \tag{16}$$

where L is the limiter output asymptotic saturation level and C is the slope of the limiter characteristic at the origin. Furthermore, if we combine the soft limiter with the 10-MHz mixer which follows it, we may treat the combination as a coherent soft limiter. Such a device was studied in Ref. 6, where it was found that for an input sinusoidal signal with an rms amplitude of A_{SL} immersed in narrow-band Gaussian noise of variance σ^2, the resulting mean output voltage μ_y is given by

$$\mu_y = L\sqrt{\frac{2R_{SL}}{\pi(1+D)}}\exp\left[\frac{-R}{2(1+D)}\right] \times \left\{I_0\left[\frac{R}{2(1+D)}\right] + I_1\left[\frac{R}{2(1+D)}\right]\right\}\cos\theta \tag{17}$$

where θ is the phase angle between the limiter input sinusoidal signal and the coherent detector reference, D is a soft limiter "softness" parameter which depends on the physical parameters of the limiter and the input noise power given by

$$D = \frac{2L^2}{\pi C^2 \sigma^2} \tag{18}$$

and R_{SL} is the soft limiter input signal-to-noise ratio given by

$$R_{SL} = \frac{A_{SL}^2}{\sigma^2} \tag{19}$$

The above expression for μ_y is valid if the detection angle θ is constant. In our case, θ is the random carrier loop phase angle $\phi_R(t)$, so that $\cos\theta$ must be replaced by its average value given in Eq. (12). If we divide Eq. (17) by the input rms amplitude and use the definition of D, we find that the equivalent gain of the coherent soft limiter is given by

$$\begin{pmatrix}\text{Equivalent soft}\\ \text{limiter gain}\end{pmatrix} = \alpha_{SL}\frac{I_1(\rho)}{I_0(\rho)}\cos\phi_{RL} \tag{20}$$

where

$$\alpha_{SL} = C\sqrt{\frac{D}{1+D}}\exp\left[-\frac{R_{SL}}{2(1+D)}\right]\left\{I_0\left[\frac{R_{SL}}{2(1+D)}\right] + I_1\left[\frac{R_{SL}}{2(1+D)}\right]\right\} \tag{21}$$

is the soft limiter average slope when the carrier tracking loop phase error is neglected.

To determine the noise at the coherent limiter output, let us define $1/\Gamma_{SL}$ as the ratio of output to input signal-to-noise density ratios. Then we have

$$\begin{pmatrix}\text{Noise}\\ \text{density}\\ \text{out}\end{pmatrix} = \Gamma_{SL}\left(\frac{\text{Signal power out}}{\text{Signal power in}}\right)\begin{pmatrix}\text{Noise}\\ \text{density}\\ \text{in}\end{pmatrix} \tag{22}$$

Since the input noise density is N_0, we have, using Eq. (20),

$$\begin{pmatrix}\text{Noise}\\ \text{density}\\ \text{out}\end{pmatrix} = \Gamma_{SL}\left[\alpha_{SL}\frac{I_1(\rho)}{I_0(\rho)}\cos\phi_{RL}\right]^2 N_0 \tag{23}$$

Now, if we define

$$K_2 = \frac{K_1(t)}{\sqrt{2}\cos\omega_c t} \tag{24}$$

we obtain the simplified mathematical model shown in Fig. 4. However, it is immediately clear that this model is the same as the one shown in Fig. 5, where we define

$$K_3 = K_2\,\alpha_{SL}\frac{I_1(\rho)}{I_0(\rho)}\cos\phi_{RL} \tag{25}$$

In order to use the above model, we must first determine expressions for D, R_{SL} and Γ_{SL}. For the Block III SDA, the virtual signal level (noise-free loop error signal level when the loop phase error is $\pi/2$) at the input to the soft limiter has a strength of +10 dBmW and the limiter saturates at a level of +4 dBmW (sinusoidal). Thus we have

$$D = \frac{0.1599\pi^2 R}{8T_S BW_{FA_2}} \tag{26}$$

where BW_{FA_2} is the one-sided noise bandwidth of the error channel bandpass filter. To determine R_{SL}, we first note from Eq. (9) that the soft limiter input is a random amplitude sine wave immersed in bandlimited Gaussian noise. If we compute the average soft limiter input signal-to-noise ratio and use the fact that

$$R = \frac{ST_S}{N_0} = \frac{A^2 \sin^2 m_{PS} T_S}{N_0} \tag{27}$$

we obtain

$$R_{SL} = \frac{4(\alpha')^2 R}{\pi^2 T_S BW_{FA_2}} [\phi^2_{SCL} + \sigma^2_{SC}] \tag{28}$$

For determining Γ_{SL}, we note that

$$\frac{1}{\Gamma_{SL}} = \frac{(SNR)_0 B_0}{2(SNR)_i B_i}$$

where $(SNR)_i$ and $(SNR)_o$ are the coherent soft limiter input and zonal output signal-to-noise power ratios, B_i is the noise bandwidth of the input bandpass filter ($= BW_{FA_2}$), B_0 is the coherent soft limiter output zonal bandwidth, and the factor of 1/2 is necessary for the bandpass-to-lowpass transformation. It was conjectured in Ref. 6 that the bandwidth ratio could be determined from the corresponding ratio for coherent hard limiters by

$$\left(\frac{B_0}{B_i}\right)_{\substack{\text{coherent}\\ \text{soft}\\ \text{limiter}}} = \frac{1}{1+D}\left(\frac{B_0}{B_i}\right)_{\substack{\text{coherent}\\ \text{hard}\\ \text{limiter}}} + \frac{D}{1+D} \tag{29}$$

where the hard limiter ratio has been experimentally determined by Springett and Simon (Ref. 8) as

$$\left(\frac{B_0}{B_i}\right)_{\substack{\text{coherent}\\ \text{hard}\\ \text{limiter}}} = 1 + \left(\frac{4}{\pi\Gamma_0} - 1\right)\exp\left[-R_{SL}\left(1 - \frac{\theta}{2}\right)\right] \tag{30}$$

with Γ_0 determined by the shape of the input bandpass filter ($= 0.862$ for ideal rectangular filter) and θ, ($0 \leq \theta \leq \pi/2$), is the coherent limiter detection reference angle as before. Again we will replace θ by an equivalent angle

$$\theta_{EQ} = \cos^{-1}\left[\frac{I_1(\rho)}{I_0(\rho)} \cos\phi_{RL}\right] \tag{31}$$

Finally, a method for computing the ratio of the soft limiter signal-to-noise power ratios is given in Ref. 6.

The remainder of the subcarrier loop analysis follows in exactly the same manner as in the Brockman papers. For example, the loop noise bandwidth is given by

$$W_{SCL} = \frac{(KK_3\tau_2^2 + \tau_1)KK_3}{2\tau_1(KK_3\tau_2 + 1)} \tag{32}$$

where τ_1 and τ_2 are the time constants of the loop filter which has a transfer function

$$F(S) = \frac{1 + \tau_2 S}{1 + \tau_1 S} \tag{33}$$

Likewise, the subcarrier loop phase error variance is given by

$$\sigma^2_{SC} = \frac{\pi^2 T_S \Gamma_{SL} W_{SCL}}{8R(\alpha')^2} \tag{34}$$

and the static phase error is

$$\phi_{SCL} = \frac{\Omega_0}{KK_3} \tag{35}$$

where Ω_0 is the subcarrier offset frequency expressed in radians/second.

It is evident at this point that the subcarrier loop equations are given parametrically in terms of the loop static phase error and phase variance. To solve these equations, a two-dimensional Newton algorithm was used to determine simultaneously the values of ϕ_{SCL} and σ^2_{SC}. The equations were found to be quite well behaved so that the solutions were obtained after just a few iterations.

III. Summary of the Results

A cursory comparison of the model presented here and the earlier Brockman model indicates a negligible difference in the effective signal strength degradation as given in Eq. (10). However, a more detailed examination shows that the two models differ when considering

(1) Low symbol rates.

(2) Subcarrier doppler offsets.

(3) Carrier tracking loop phase errors.

We shall examine each of these in more detail.

A. Low Symbol Rates

At low symbol rates, the signal-to-noise spectral density ratio S/N_0 is generally quite small and usually results in

an increase in subcarrier loop phase noise. In the model presented here, this phase noise affects the loop equations to further degrade the loop performance. Comparisons of signal-to-noise ratio degradations for the two models at design point symbol rates are shown in Figs. 6–8.

B. Subcarrier Doppler Offsets

When the received subcarrier frequency differs from the value established by the SDA synthesizer, a static phase error (SPE) results within the subcarrier loop. Previous models have predicted that this error is a linear function of subcarrier offset frequency. In the above model, the subcarrier phase error is allowed to degrade (reduce) data limiter gain α'. At the same time, the SPE causes an increase in soft limiter input signal which, in turn, causes a reduction in the soft limiter gain. These gain reductions have the effect of diminishing the ability of the subcarrier loop to track doppler, which further increases the SPE. The result is that the SPE is related to the offset frequency in a parabolic manner as shown in Fig. 9.

Another quantity affected by subcarrier offsets is the loop phase jitter. The reduction of α' and α_{SL} causes the loop bandwidth to decrease. At the same time, the increased loop error signal causes Γ_{SL} to decrease. However, at low signal-to-noise ratios, the reduction of α' occurs at a sufficiently fast rate to override the decreasing $\Gamma_{SL} W_{SCL}$ product so that the jitter increases. On the other hand, when the SNR is high the reduction of α' occurs much more slowly and results in a decreasing phase jitter. These variations in phase jitter, however, are quite small and for most purposes can be neglected.

C. Carrier Tracking Loop Phase Errors

When carrier tracking errors occur, the subcarrier loop gain is decreased directly at the error channel IF mixer as well as indirectly through α' and renders the loop more susceptible to doppler shift. The subcarrier phase jitter is also affected by tracking errors in a manner similar to that when doppler offsets exist. The main difference between the two is that when tracking errors exist the SDA jitter increases only when both the signal-to-noise ratio and the symbol rate are low. This occurs because the SDA phase jitter is small at high symbol rates (regardless of SNR) and hence produces little degradation of α'. As before, these variations in the value of jitter are extremely small and, for most practical purposes, can be neglected.

References

1. Brockman, M. H., "MMT Subcarrier Demodulator," SPS 37-46, Vol. III, Jet Propulsion Laboratory, Pasadena, Calif., July 1967, pp. 189–204.
2. Brockman, M. H., "Analysis of the Subcarrier Demodulator," SPS 37-48, Vol. II, Jet Propulsion Laboratory, Pasadena, Calif., November 1967, pp. 124–129.
3. Brockman, M. H., "Subcarrier Demodulator Analysis," SPS 37-49, Vol. II, Jet Propulsion Laboratory, Pasadena, Calif., January 1968, pp. 100–113.
4. Brockman, M. H., "MMTS: Performance of the Subcarrier Demodulator," SPS 37-52, Vol. II, Jet Propulsion Laboratory, Pasadena Calif., July 1968, pp. 127–141.
5. Brockman, M. H., "An Efficient and Versatile Telemetry Subcarrier Demodulation Technique for Deep Space Telecommunications," Proc. 4th Hawaiian International Conference on System Science, January 1971.
6. Lesh, J. R., "Signal to Noise Ratios in Coherent Soft Limiters," submitted to *I.E.E.E. Transactions on Communications.*
7. Lindsey, W. C., "Performance of Phase-Coherent Receivers Preceded by Bandpass Limiters," *I.E.E.E. Trans. Comm. Tech.*, Vol. Comm 16, No. 2, pp. 245–251, April 1968.
8. Springett, J. C., and Simon, M. K., "An Analysis of the Phase Coherent-Incoherent Output of the Bandpass Limiter," *I.E.E.E. Trans. Comm. Tech.*, Vol. Comm. 19, No. 1, pp. 42–49, February 1971.

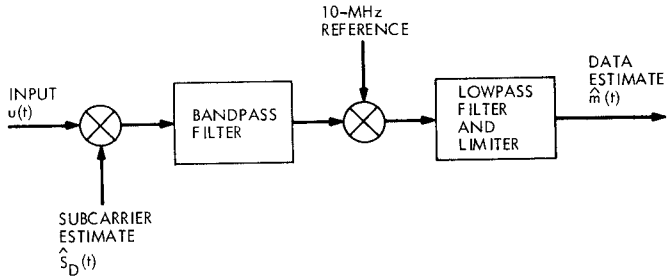

Fig. 1. Block diagram, SDA data channel

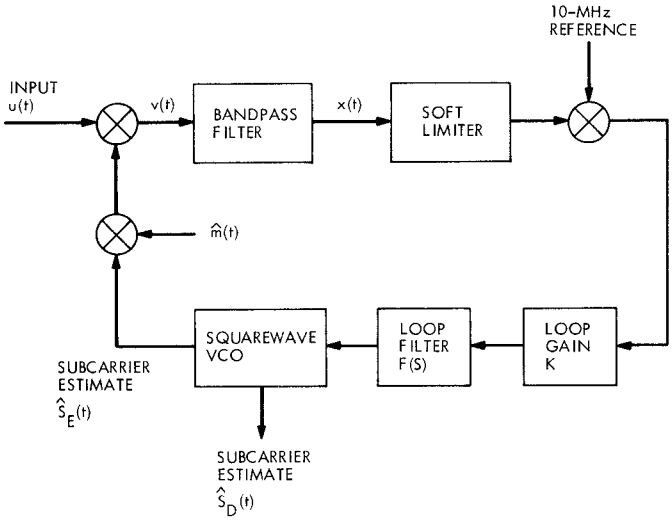

Fig. 2. Block diagram, SDA error channel

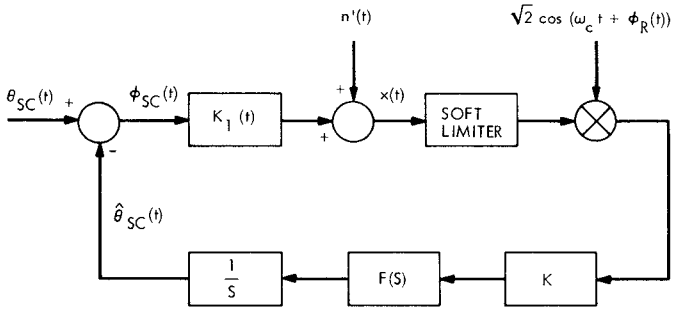

Fig. 3. Mathematical model, SDA error channel

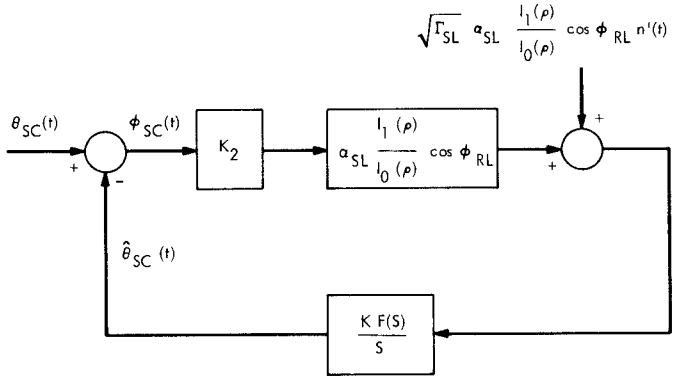

Fig. 4. Reduced mathematical model

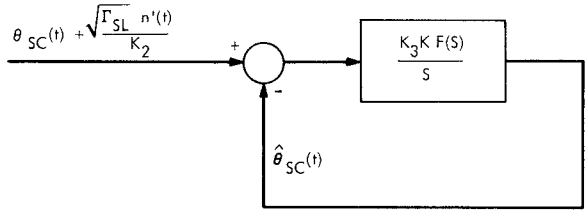

Fig. 5. Simplified mathematical model

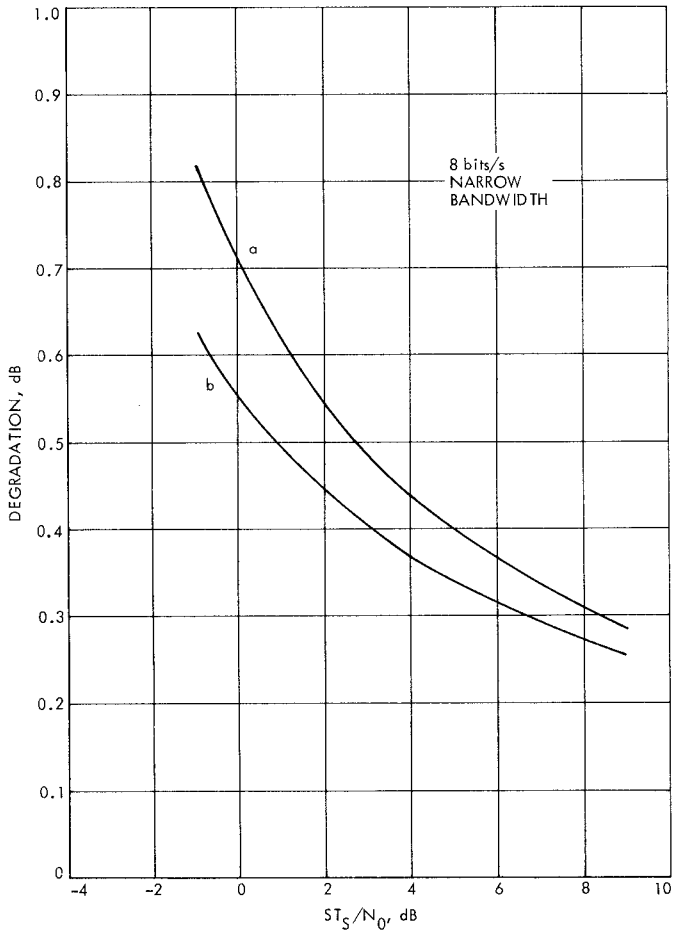

Fig. 6. SNR degradation, (a) new model, (b) previous model, at 8 bits/s

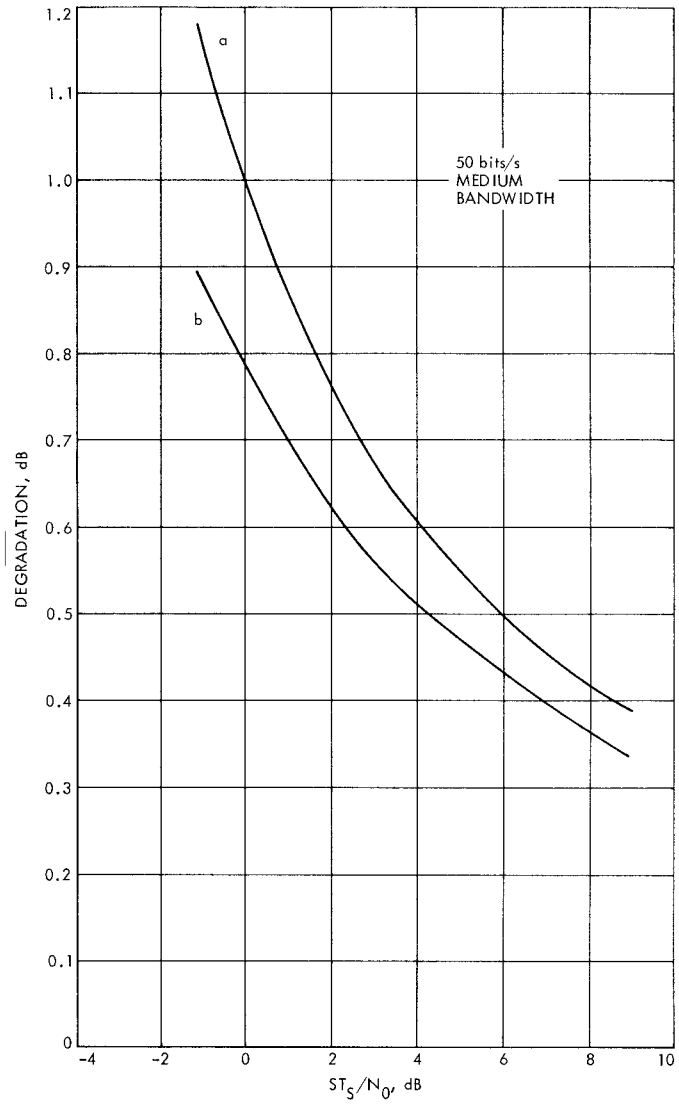

Fig. 7. SNR degradation, (a) new model, (b) previous model, at 50 bits/s

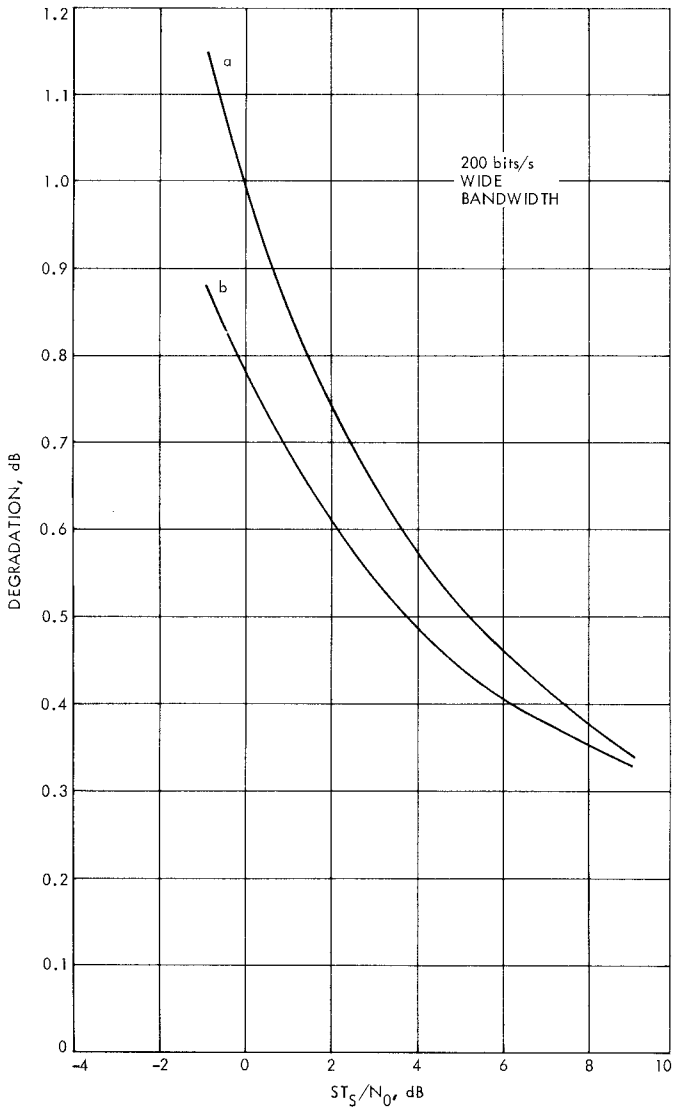

Fig. 8. SNR degradation, (a) new model, (b) previous model, at 200 bits/s

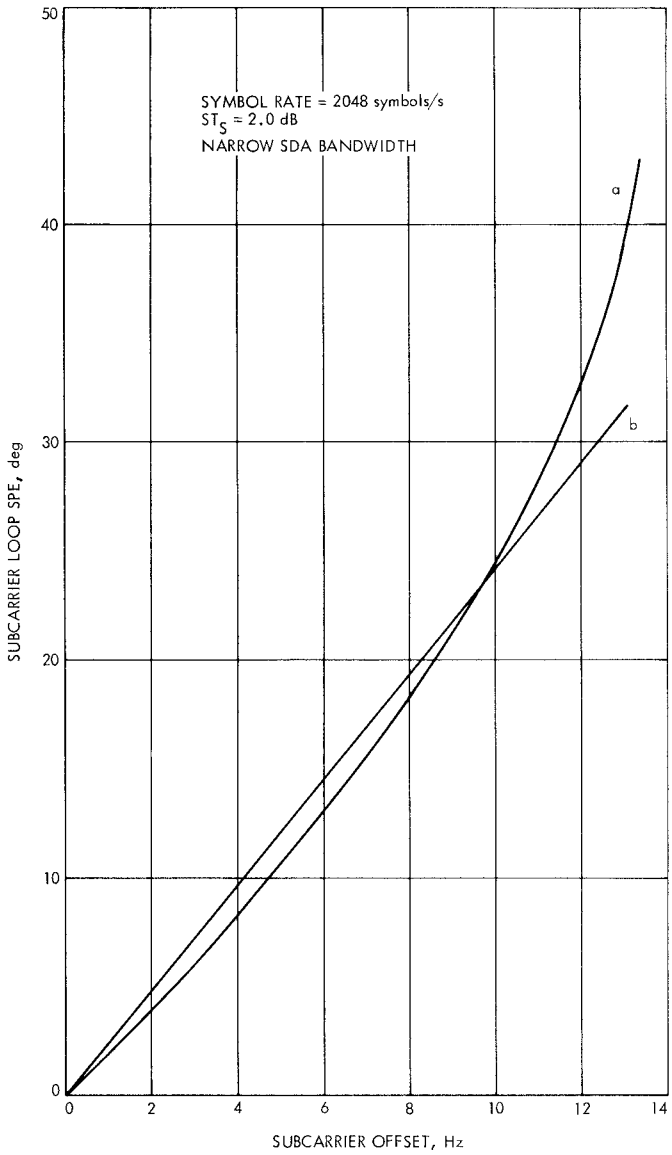

Fig. 9. Static phase error vs subcarrier offset for (a) new model, (b) previous model